Hindawi
Complexity
Volume 2019, Article ID 3745924, 14 pages
https://doi.org/10.1155/2019/3745924

Research Article

Multiobjective Optimal Control for Hydraulic Turbine Governing System Based on an Improved MOGWO Algorithm

Xin Xia,[1] **Jie Ji**,[1] **Chao-shun Li**,[2] **Xiaoming Xue**,[1] **Xiaolu Wang**,[1] **and Chu Zhang**[1]

[1]*College of Automation, Huaiyin Institute of Technology, Huaian 223003, China*
[2]*College of Hydroelectric Digitization Engineering, Huazhong University of Science and Technology, Wuhan 430074, China*

Correspondence should be addressed to Jie Ji; j.ji2@newcastle.ac.uk

Received 3 January 2019; Revised 9 April 2019; Accepted 22 April 2019; Published 28 May 2019

Academic Editor: Matilde Santos

Hydraulic turbine governing system (HTGS) is essential equipment which regulates frequency and power of the power grids. In previous studies, optimal control of HTGS is always aiming at one single operation condition. The variation of operation conditions of HTGS is seldom considered. In this paper, multiobjective optimal function is proposed for HTGS under multiple operation conditions. In order to optimize the solution to the multiobjective problems, a novel multiobjective grey wolf optimizer algorithm with searching factor (sMOGWO) is also proposed with two improvements: adding searching step to search more no-domain solutions nearby the wolves and adjusting control parameters to keep exploration ability in later period. At first, the searching ability of the sMOGWO has been verified on several UF test problems by statistical analysis. And then, the sMOGWO is applied to optimize the solutions of the multiobjective problems of HTGS, while different algorithms are employed for comparison. The experimental results indicate that the sMOGWO is more effective algorithm and improves the control quality of the HTGS under multiple operation conditions.

1. Introduction

With the increase of people's consciousness of environmental protection, more and more renewable energy has been applied to replace the traditional energy, such as wind power [1, 2] and solar power [3]. As wind power and solar power are connected with the large-scale power grid, people want to maximally utilize renewable energy on the premise that power balance is maintained [4–6]. However, the output of wind power and solar power is not steady due to the intermittent and fluctuating nature. Therefore the power grid needs regulating equipment to keep power balance. As the hydroelectric unit is easier for changing the output power, it has been widely used as power and frequency regulating equipment in power grid [7, 8].

Hydraulic turbine governing system (HTGS) which mostly contains PID controller is important automatic control equipment of hydroelectric unit [9]. The HTGS can adjust the output power of hydroelectric unit by changing the opening of guide. Therefore the control quality of HTGS influences the regulation quality of hydroelectric unit directly.

Many research works have been done to improve the control quality; these works can be mainly divided into two categories: proposed new control models instead of PID controller and optimized control parameters of HTGS. In [10], a fractional order PID controller, whose order of derivative portion and integral portion is not integer, is proposed for HTGS. The fractional order PID controller provides more flexibility in achieving control objective. In [11], a fuzzy-PID controller is designed to improve control quality of HTGS. In [12], the sliding mode variable structure control strategy led to HTGS which has better robustness and adaptability than PID controller. In [13], a new adaptive inverse control method based on the learning characteristic of neural network was proposed for HTGS to improve the dynamic and stationary performance. All the above control models are useful, but they ignore that it is hard to change the control device to reach the control models for most operating hydroelectric units. Thus control parameter optimization seems more suitable to improve control quality for actual situation. To optimize PID controller, some popular optimization algorithms, including genetic algorithm (GA) [14], particle swarm optimization

(PSO) [15], gravitational search algorithm (GSA) [16, 17], and ant lion optimization (ALO) [18], have been successfully applied in parameter optimization of HTGS. All these algorithms optimize the PID parameters by optimizing one objective function which means the optimal parameters are under one single operating condition; few of the researches have taken multiple operation conditions into consideration. The optimal results may not be suitable for variation of operation conditions of HTGS. Therefore, the study on parameter optimal control of HTGS under multiple operation conditions is meaningful and challengeable.

Parameter optimal control of HTGS under multiple operation conditions actually refers to the multiobjective optimization problems. Some multiobjective optimization algorithms have been proposed and successfully applied in various applications in decades [19–25], such as nondominated sorting genetic algorithm II (NSGA-II) [19], multiobjective evolutionary algorithm based on decomposition (MOEA/D) [21], the strength Pareto evolutionary algorithm (PESA-II) [22], multiobjective particle swarm optimization (MOPSO) [23], and the multiobjective grey wolf optimizer (MOGWO) [25]. Among these multiobjective optimization algorithms, MOGWO algorithm has proved to be effective in multiobjective optimization problems than other algorithms [25]. However, as the guidance of lead wolves is much greater than the random factor, this algorithm is easy to fall into local optimum and has poor stability. Therefore it is necessary to enhance the searching ability of MOGWO.

The main contribution of this paper is the design and optimization of HTGS under multiple operation conditions by using an improved MOGWO algorithm. Firstly, the problem in optimal control of HTGS is explained and multiobjective optimal function is proposed. Secondly, a novel MOGWO algorithm based on searching factor (sMOGWO) is proposed to optimize the multiobjective problem. The sMOGWO is expected to improve the searching ability of MOGWO from two aspects: adding searching step to search more no-domain solutions nearby the wolves and adjusting control parameters to keep exploration ability in later period.

The remaining part of this paper is organized as follows: the HTGS model and its control problem are discussed in Section 2. In Section 3, the weakness of MOGWO algorithm is analyzed and an improved MOGWO algorithm is proposed. In Section 4, simulation verification is present to demonstrate the advantage of the proposed sMOGWO algorithm compared with MOGWO, MOPSO, and other popular multiobjective evolutionary algorithms. Section 5 illustrates the case study and results along with a few discussions. Finally, conclusions from this research as well as the advantages and limitations of the proposed algorithm are discussed in Section 6.

2. HTGS Model and Its Control Problems

2.1. The HTGS Model. The HTGS is essential equipment of the hydropower station. The HTGS contains PID controller, electrohydraulic servo system, hydroturbine, and hydrogenerator.

The PID controller has been widely used in HTGS. In this paper, the structure of the PID controller model and electrohydraulic servo system is set as in Figure 1. Many nonlinear factors have been considered in the electrohydraulic servo system, such as the dead zone and the relay device limiting, where x_r is the frequency giving; x_u is the disturbance frequency; x is the frequency of the hydrogenerator unit; k_p, k_d, k_i are the proportionality coefficient, differential coefficient, and integration coefficient, respectively; T_{1v} is the differential filtering time constant; b_p is the permanent difference coefficient; T_y is the response time constant of main control valve; and y represents the gate opening.

The hydroturbine is a complex system with strong nonlinear and time-varying character. Generally, the hydroturbine model can be descripted as follows:

$$\begin{aligned} m_t &= m_t(y, h, \omega) \\ q &= q(y, h, \omega) \end{aligned} \tag{1}$$

where m_t is the hydraulic machinery power, q is discharge of hydraulic turbine, y represents the gate opening, ω represents speed of hydraulic turbine, and h represents the water head.

In this paper, the little fluctuation in transient of hydraulic power station is researched; the model of hydraulic turbine can be described as liner model, as follows:

$$\begin{aligned} m_t &= e_x\omega + e_y y + e_h h \\ q &= e_{qx}\omega + e_{qy} y + e_{qh} h \end{aligned} \tag{2}$$

where e_h is the transfer coefficient of turbine torque on the water head, e_y is the transfer coefficient of turbine torque on the guide leaf opening, e_x is the transfer coefficient of turbine torque on the speed, e_{qx} is the transfer coefficient of turbine flow on the speed, e_{qy} the transfer coefficient of turbine flow on guide leaf opening, and e_{qh} is the transfer coefficient of turbine flow on the water head.

In water diversion system, the water hammer and pipe wall can be considered as rigid under small fluctuations. The transfer function of rigid water diversion system can be expressed as

$$G_r(s) = -T_w s \tag{3}$$

where T_w is the water inertia time constant.

In this paper, the core problem is the dynamic response of the HTGS. Hence, the dynamic speed of the generator is considered. The model of the generator can be described as the following transfer function:

$$\frac{x}{m_t} = \frac{1}{T_a s + e_g} \tag{4}$$

where x represents the frequency of the hydrogenerator unit, T_a represents the inertia time constant, and e_g is the adaptive control coefficient.

As in the above description of the mathematical model, the hydrogenerator unit model can be described as the block diagram in Figure 2.

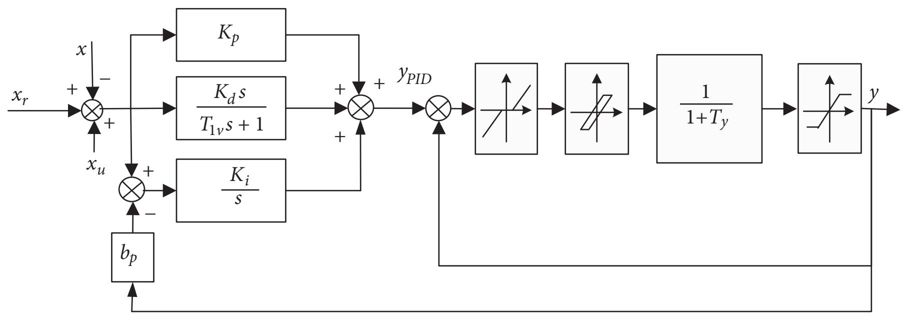

FIGURE 1: PID control device and electric-hydraulic servo system.

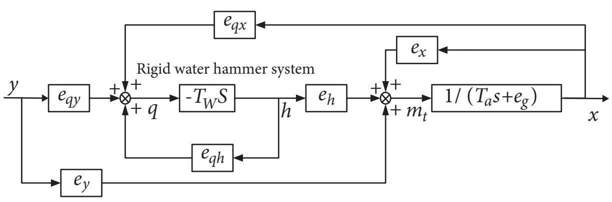

FIGURE 2: Hydroturbine unit model with rigid water hammer.

2.2. Optimal Control of HTGS and Problems Analysis. The performance indexes of the optimal control of the HTGS are the most direct measure to evaluate the control quality. Therefore, the optimal control of the HTGS is the optimal control of performance indexes. The objective functions of optimal control are formed by a certain performance index or several performance indexes in most researches. The performance indexes in HTGS can be mainly divided into the following two categories [26]:

(i) Performance indexes for the transition process mainly include adjusting time, rising time, steady state error, and overshoot.

(ii) Performance indexes of error functional integral mainly include integral time absolute error (ITAE), integral absolute error (IAE), integral square time absolute error (ISTAE), integral square time square error (ISTSE), integral time square error (ITSE), and integral square error (ISE).

The performance indexes of error functional integral are comprehensive indexes which make optimal control easier to meet the control requirements. The ITAE is one of the most widely used which has the characteristics of steady adjustment and small overshoot.

Many researches have been done for optimal control of HTGS by optimizing ITAE. However most of the researches are for one single operation condition. As the hydrogenerator usually plays the roles of generating electricity, peak modulation, frequency modulation, and voltage modulation, there is a variety of operation conditions and frequent changes. The optimal control parameters may not be suitable for all the operation conditions.

Here, we will give an example to explain this problem. Parameters of two classical operation conditions of the above HGTS model are given as follows:

No-load: T_{y1}=0.02s, T_y=0.1s, T_w=0.66s, T_{1v}=0.28, T_a=8.51s, b_p=0.01, e_g=1, e_h=0.508, e_y=0.903, e_x=-0.242, e_{qx}=0.634, e_{qy}=-0.396, e_{qh}=0.261.

On-load: T_{y1}=0.02s, T_y=0.1s, T_w=0.66s, T_{1v}=0.28, T_a=8.51s, b_p=0, e_g=1, e_h=1.34, e_y=0.926, e_x=-1.184, e_{qx}=0.371, e_{qy}=0.974, e_{qh}=0.308.

5% step disturbance is set for HGTS. The optimal control parameters of HTGS under no-load condition are acquired by optimizing ITAE. The parameters are K_p=14.665, K_i=3.026, and K_d=0. The control transient process is shown in Figure 3. The control effect is well. However, if the parameters are used for the on-load condition, it is an ineffective control strategy.

The result indicates that the optimal control parameters of one single operation condition cannot be suitable for all the operation conditions. Accordingly, the optimal control of HTGS is a multiobjective optimization problem in fact. In this paper, we have proposed a novel control parameters optimization objective function. Different operation conditions are considered for optimal control. Because the no-load and on-load are the extreme operating conditions, the ITAE of both conditions are the objective functions. The objective function can be described as follows:

$$\begin{aligned} \min \quad & J_1 = ITAE_{no-load} = f_1\left(K_p, K_i, K_d, y\right) \\ & J_2 = ITAE_{on-load} = f_2\left(K_p, K_i, K_d, y\right) \end{aligned} \tag{5}$$

$$\begin{aligned} \textit{subject to} \quad & 0 \le K_p \le 15 \\ & 0 \le K_i \le 15 \\ & 0 \le K_d \le 5 \\ & 0 \le y \le 1 \end{aligned} \tag{6}$$

where f_1 and f_2 represent the relationship between the parameters and the ITAE. Equation (6) represents the range of parameters.

3. An Improved MOGWO Algorithm

MOGWO algorithm as a new intelligent optimization algorithm has a better convergence rate than other intelligent optimization algorithms. Therefore, it has received great attention and wide application since it has been proposed.

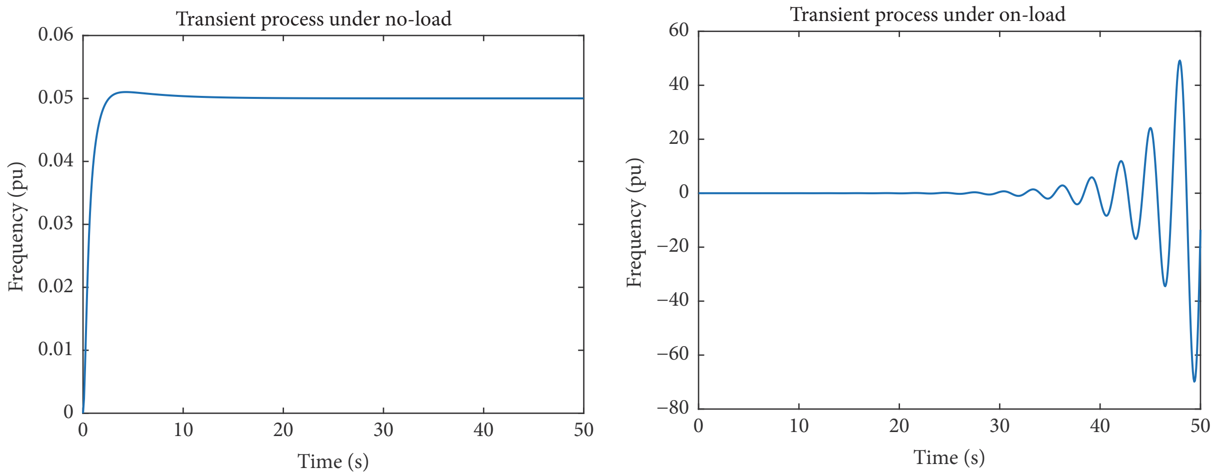

Figure 3: Transient process by different control strategies.

3.1. Grey Wolf Optimizer and MOGWO Algorithm. The grey wolf optimizer (GWO) algorithm proposed by Mirjalili et al. in 2014 is a new intelligent optimization algorithm mimicking the hierarchies and hunting strategies of wolves [27]. In GWO, each grey wolf is treated as a potential solution. The grey wolves at the best solution, the second best solution, and the third best solution are treated as α, β, and δ wolves. The rest of the grey wolves are treated as ω wolves. The wolves are approaching the food position (global optimal solution) according to the guidance of α, β, and δ wolf. The equations that simulate the guidance of hunting are as follows:

$$\mathbf{D} = \left|\mathbf{C} \cdot \mathbf{X}_p(t) - \mathbf{X}(t)\right| \tag{7}$$

$$\mathbf{X}(t+1) = \mathbf{X}_p(t) - \mathbf{A} \cdot \mathbf{D} \tag{8}$$

where $\mathbf{X}$ represents the position vector of a grey wolf, $\mathbf{X}_p$ represents the position vector of the prey, and t represents the current iteration. $\mathbf{A}$ and $\mathbf{C}$ are coefficient vectors subject to the following equations:

$$\mathbf{A} = 2 \cdot \mathbf{a} \cdot \mathbf{r}_1 - \mathbf{a} \tag{9}$$

$$\mathbf{C} = 2 \cdot \mathbf{r}_2 \tag{10}$$

where $\mathbf{r}_1$ and $\mathbf{r}_2$ are random vectors from 0 to 1. $\mathbf{a}$ is control parameter from 2 to 0 and it will linearly decrease as the number of iterations increases.

In 2016, Mirjalili proposed a multiobjective GWO algorithm named 'MOGWO algorithm' for multiobjective problems. There are two major changes in MOGWO: using the external population Archive to store the current nondominated solutions and proposing a selection strategy for multiobjective optimization.

3.2. sMOGWO Algorithm. Although the MOGWO algorithm has a better convergence rate, it is easy to fall into local optimum and has poor stability. The main reasons are summarized as follows:

(i) The algorithm has great randomness only when initializing the position of wolves. Even though there is random factor in algorithm, when the position of wolves is updated, the effect of the guidance of lead wolves is much greater than the random factor. Thus the algorithm is highly dependent on the initial value, and self-regulation ability is weak.

(ii) The MOGWO algorithms select α, β, and δ wolves from Archive. However, if Archive set falls into local optimum, the algorithms can hardly skip the local optimum. Therefore, the exploration ability of the algorithm needs to be improved at later period of the optimization.

As the guidance of lead wolves has too much influence, the grey wolves always blindly follow the lead wolves and the nondominated solutions around the lead wolves. The grey wolves always ignore the nondominated solutions beside them. Actually, the grey wolves often pass nearby other nondominant solutions when following the lead wolves. If the grey wolves have the ability of independent searching, the global optimization ability of the algorithm will be greatly improved.

Consequently, in this paper, we proposed to add the searching factor in MOGWO named 'sMOGWO algorithm'. After the position updating of wolves, the wolves will have the searching step. Each wolf will search the nearby position randomly; if the nearby position is better than the current position, the wolf will move to the new position. The step can be described as the following mathematical expressions:

$$\Delta(x_1, x_2, \cdots x_{\dim}) = \begin{cases} x_k = r \cdot (ub_k - lb_k), & k = \mathrm{rand}\{1, 2, \cdots \dim\} \\ x_i = 0, & i = 1, 2, \cdots \dim \textit{ and } i \neq k \end{cases} \tag{11}$$

$$\mathbf{X}_{searching} = \mathbf{X} + \Delta \tag{12}$$

$$\begin{aligned} &\mathbf{X}_{new} = \mathbf{X}_{searching}, \quad \text{if } f\left(\mathbf{X}_{searching}\right) \succ f(\mathbf{X}) \\ &\mathbf{X}_{new} = \mathbf{X}, \quad \textit{otherwise} \end{aligned} \tag{13}$$

where Δ is the searching step of the wolf, r is a random number between -0.5 and 0.5, ub_k and lb_k are the upper and lower boundary of x_k, dim is the dimension of wolf, $\mathbf{X}$ is the

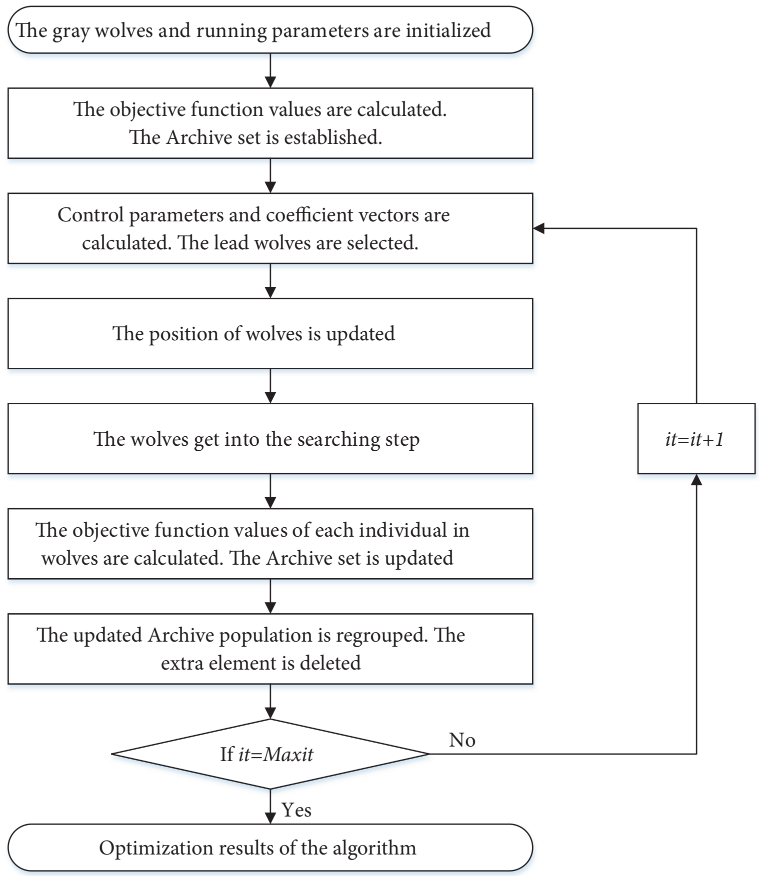

Figure 4: The flow chart of the sMOGWO algorithm.

position of the wolf, $\mathbf{X}_{new}$ is the new position after searching, and $\succ$ represents the dominance relationship.

In the original algorithm, the control parameter a linearly decreases as the number of iterations increases to keep high exploration ability at early period and high exploitation ability at later period. However, there is higher demands for exploration ability in multiobjective optimization. Therefore, in this paper, the control parameter a is also modified. The adjustment strategy of control parameter a must be subject to the following:

$$\begin{gathered} a = 2 - 2 \cdot f(x), \\ x = \frac{it}{Maxit} \in [0.1] \\ f(0) = 0, \\ f(1) = 1 \end{gathered} \tag{14}$$

where *Maxit* is the maximum number of iterations and $f(x)$ is a monotone increasing function, in original algorithm $f(x)=x$.

The higher the value of a, the stronger the exploration ability of the algorithm, so the $f(x)$ should be a concave function among $[0, 1]$. Here, we proposed to use the following equation for control parameter a.

$$a = 2 - 2 \cdot \left(\frac{it}{Maxit}\right)^2 \tag{15}$$

The flow chart of the sMOGWO algorithm is shown in Figure 4.

The steps of the sMOGWO algorithm are as follows.

Step 1. Archive size is N_A, population size of grey wolves is N, number of grids per dimension is *dim*, inflation rate is a, and maximum number of iterations is *Maxit*. Leader selection pressure and deletion selection pressure are also set. The grey wolves and running parameters are initialized.

Step 2. The objective function values of each individual wolf are calculated. The Archive set is established, and the Archive population is grouped into iterative process.

Step 3. The $\overrightarrow{A}$, $\overrightarrow{C}$, and a are calculated according to (9), (10), and (15); then the lead wolves are selected.

Step 4. The position of wolves is updated according to (7) and (8).

Step 5. The wolves get into the searching step according to (11), (12), and (13)

Step 6. The objective function values of each individual in wolves are calculated. The nondominant solutions of wolves are compared to the individuals in the Archive population one by one, and the Archive set is updated.

Step 7. The updated Archive set is regrouped and the number of individuals in the Archive population is checked. If the number of individuals exceeds the maximum of population, the extra solutions will be deleted.

Step 8. The algorithm ends when the maximum number of iterations is reached. All individuals in the Archive population are the optimization results of the algorithm. Otherwise, the algorithm returns back to Step 3.

3.3. Computational Complexity Analysis. The computational complexity of MOGWO and sMOGWO is analyzed in this part.

The computational complexity of each iteration (Step 3 to Step 7) of the iterative process is analyzed one by one. The number of individuals in the current Archive set is A, the number of individuals in the grey wolf population is N, and the dimension of each individual is dim.

In Step 3, lead wolves are selected by calculating the roulette probability for each individual in the Archive set. The computational complexity can be expressed as $\mathrm{O}(A)$.

In Step 4, the computational complexity of position updating can be expressed as $\mathrm{O}(N*dim)$.

In Step 5, the objective function values need be calculated by searching step, and the computational complexity can be expressed as $\mathrm{O}(N*dim)$.

In Step 6, the nondominant solutions of wolves are compared to the individuals in the Archive set one by one to update the Archive set. The computational complexity is $\mathrm{O}(A*N*dim)$.

In Step 7, the Archive sets are grouped and sorted, and the computational complexity is $\mathrm{O}(A^2)$.

The computational complexity of sMOGWO in each iteration is $\mathrm{O}(A^2)+\mathrm{O}(A*N*dim)$. The MOGWO includes all the above steps expect Step 5, and the computational complexity of MOGWO is also $\mathrm{O}(A^2)+\mathrm{O}(A*N*dim)$. The proposed modified method has the same computational complexity as the original method. In addition, although an additional Step 5 is added to the sMOGWO algorithm, it can effectively reduce Archive set with a large number of similar nondominant solutions, which has great influence on the computational complexity. In fact, the proposed method can reduce the optimization time.

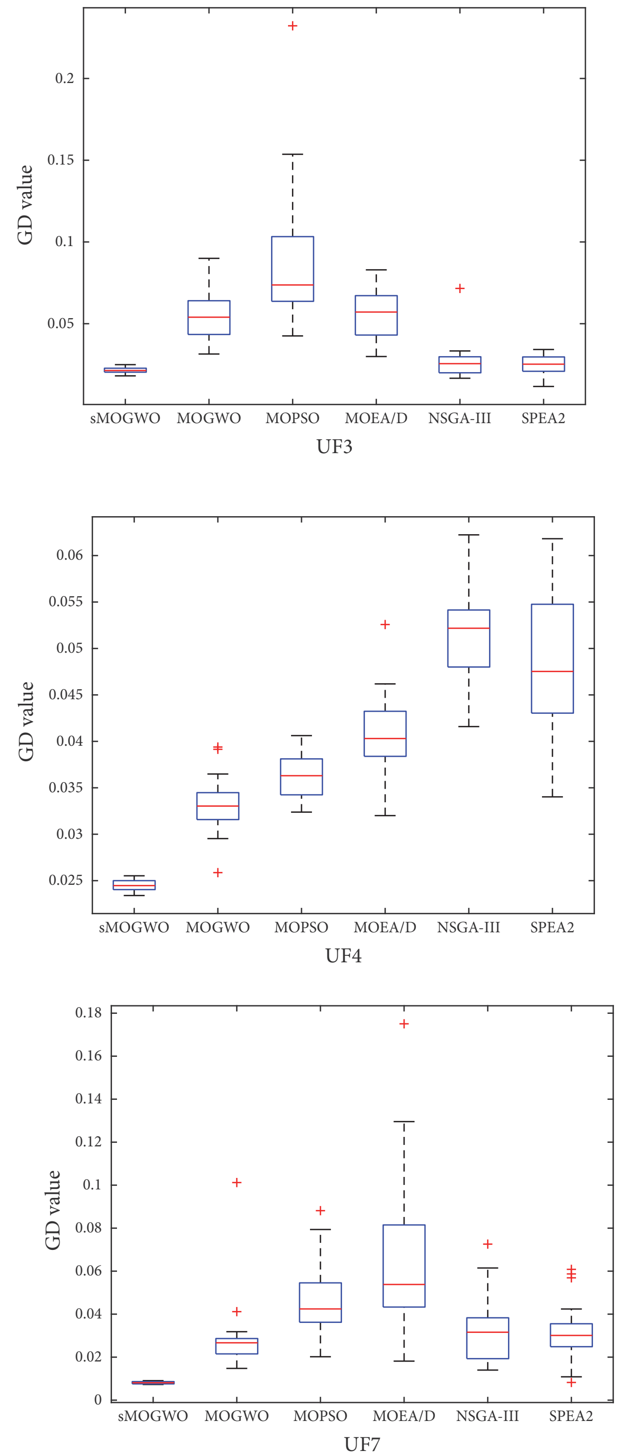

Figure 5: The boxplots of GD value of three algorithms.

4. Simulation Verification

In this section, simulation verification is present to demonstrate the advantage of the proposed sMOGWO algorithm. The proposed algorithm is compared to the MOGWO algorithm [25] and some other popular multiobjective optimal algorithms [28]: MOPSO, NSGA-III, MOEA/D, and SPEA2.

4.1. Test Problems. UF series test problems in CEC 2009 are multimode test functions [29], and there are a lot of locally optimal solutions, so it is suitable for test of multiobjective optimal algorithms. Three typical test problems are chosen as

Table 1: The parameters of different multiobjective optimization algorithms.

Description	sMOGWO	MOGWO	MOPSO	NSGA-III	MOEA/D	SPEA2
Maximum number of iterations	1000	1000	1000	1000	1000	1000
Population size	*nPop*=100	*nPop*=100	*nPop*=100	*nPop*=100	*nPop*=100	*nPop*=100
Archive size	100	100	100	100	100	100
Inflation rate	α=0.1	α=0.1	α=0.1	/	/	/
Number of grids per dimension	*nGrid*=10	*nGrid*=10	*nGrid*=10	/	/	/
Leader selection pressure	β=4	β=4	β=4	/	/	/
Deletion selection pressure	γ=2	γ=2	γ=2	/	/	/
Inertia weight	/	/	ω=0.5	/	/	/
Inertia weight damping rate	/	/	ω_{damp}=0.99	/	/	/
Mutation rate	/	/	*mu*=0.1	*mu*=0.1	*mu*=0.1	*mu*=0.1
Crossover rate	/	/	/	0.5	0.5	0.5
Number of Neighbors	/	/	/	/	10	/

Table 2: Statistical results of GD for different algorithms.

GD		sMOGWO	MOGWO	MOPSO	NSGA-III	MOEA/D	SPEA2
UF3	Mean	0.0210	0.0542	0.0853	0.0268	0.0561	0.0254
	Med	0.0211	0.0540	0.0737	0.0255	0.0571	0.0252
	Max	0.0253	0.0900	0.2322	0.0716	0.0829	0.0342
	Min	0.0180	0.0315	0.0425	0.0166	0.0299	0.0116
UF4	Mean	0.0239	0.0331	0.0361	0.0516	0.0409	0.0485
	Med	0.0241	0.0330	0.0363	0.0521	0.0439	0.0475
	Max	0.0257	0.0394	0.0406	0.0622	0.0526	0.0618
	Min	0.0234	0.0259	0.0324	0.0415	0.0320	0.0340
UF7	Mean	0.0078	0.0267	0.0468	0.0319	0.0802	0.0313
	Med	0.0077	0.0278	0.0424	0.0316	0.0584	0.0301
	Max	0.0091	0.1012	0.0881	0.0726	0.1751	0.0608
	Min	0.0072	0.0148	0.0202	0.0140	0.0182	0.0082

follows: UF3 whose Pareto boundary is concave shape, UF4 whose Pareto boundary is convex shape, UF7 whose Pareto boundary is line. The three UF problems are as follows:

UF3 problem, n=30, the search space is $[0,1]^n$:

$$\begin{aligned}
\min \quad & f_1 = x_1 + \frac{2}{|J_1|}\left(4\sum_{j\in J_1} y_j^2 - 2\prod_{j\in J_1}\cos\left(\frac{20y_i\pi}{\sqrt{j}}\right) + 2\right) \\
& f_2 = 1-\sqrt{x_1} + \frac{2}{|J_1|}\left(4\sum_{j\in J_1} y_j^2 - 2\prod_{j\in J_1}\cos\left(\frac{20y_i\pi}{\sqrt{j}}\right) + 2\right) \\
\textit{subject to} \quad & y_i = x_j - x_1^{0.5(1+3(j-2)/(n-2))}, \quad j = 2,\ldots,n, \\
& J_1 = \{j \mid j \text{ is odd and } 2 \le j \le n\} \\
& J_2 = \{j \mid j \text{ is even and } 2 \le j \le n\}
\end{aligned} \tag{16}$$

UF4 problem, n=30, the search space is $[0,1]\times[-2,2]^{n-1}$:

$$\begin{aligned}
\min \quad & f_1 = x_1 + \frac{2}{|J_1|}\sum_{j\in J_1} h(y_i) \\
& f_2 = 1 - x_1^2 + \frac{2}{|J_2|}\sum_{j\in J_1} h(y_i) \\
\textit{subject to} \quad & y_i = x_j - \sin\left(6\pi x_1 + \frac{j\pi}{n}\right), \quad j = 2,\ldots,n, \\
& h(t) = \frac{|t|}{1+e^{2|t|}} \\
& J_1 = \{j \mid j \text{ is odd and } 2 \le j \le n\} \\
& J_2 = \{j \mid j \text{ is even and } 2 \le j \le n\}
\end{aligned} \tag{17}$$

Table 3: Statistical results of SP for different algorithms.

SP		sMOGWO	MOGWO	MOPSO	NSGA-III	MOEA/D	SPEA2
UF3	Mean	0.5719	1.0807	0.9091	1.0130	1.0233	0.9992
	Med	0.53456	1.1129	0.9073	1.0000	1.0196	0.9993
	Max	0.7215	1.4434	1.0411	1.0850	1.0747	1.0002
	Min	0.4490	0.6002	0.7810	0.9991	1.0000	0.9971
UF4	Mean	0.6098	0.8207	0.7923	0.9991	1.2974	1.5026
	Med	0.6217	0.8055	0.7707	0.9940	1.2924	1.4754
	Max	0.6551	1.0963	0.9160	1.0616	1.4337	1.9870
	Min	0.5428	0.6724	0.6908	0.9464	1.1553	1.1513
UF7	Mean	0.6646	0.8731	0.8649	1.0961	1.0697	0.9995
	Med	0.6646	0.8592	0.8386	1.0850	1.0015	0.9996
	Max	0.7011	1.2232	1.0611	1.2400	1.5393	1.0760
	Min	0.6186	0.5954	0.7292	0.9997	1.0000	0.9553

UF7 problem, n=30, the search space is $[0,1] \times [-1,1]^{n-1}$:

$$\begin{aligned}
\min \quad & f_1 = \sqrt[5]{x_1} + \frac{2}{|J_1|} \sum_{j \in J_1} y_i^2 \\
& f_2 = 1 - \sqrt[5]{x_1} + \frac{2}{|J_2|} \sum_{j \in J_1} y_i^2 \\
\textit{subject to} \quad & y_i = x_j - \sin\left(6\pi x_1 + \frac{j\pi}{n}\right), \\
& \qquad j = 2, \ldots, n, \\
& J_1 = \{ j \mid j \text{ is odd and } 2 \le j \le n \} \\
& J_2 = \{ j \mid j \text{ is even and } 2 \le j \le n \}.
\end{aligned} \tag{18}$$

4.2. Parameters Setting. The principles and the operation modes of the algorithms are different. In order to make the algorithm contrast, the same maximum number of iterations, population size, and Archive size are set up. The parameters of different multiobjective optimization algorithms are shown in Table 1.

4.3. Performance Evaluation Indexes. The Generational Distance (GD) and the Spacing (SP) [30] have been used to evaluation the performance of each algorithm.

$$GD = \frac{1}{N} \sqrt{\sum_{i=1}^{N} {D_i}^2} \tag{19}$$

where D_i is the Euclidean distance between the ith nondominant solution in Pareto solution set and the closest nondominant solution on the real Pareto front. N is the number of Pareto optimal solutions. The smaller value of GD indicates that the Pareto optimal solution is closer to the real Pareto front.

$$SP = \frac{d_f + d_l + \sum_{i=1}^{N-1} \left| d_i - \overline{d} \right|}{d_f + d_l + (N-1) \cdot \overline{d}} \tag{20}$$

where d_i is the Euclidean distance between the adjacent points of Pareto optimal solution. d_f and d_l are the Euclidean distances between the endpoint of Pareto optimal solution and real Pareto front. N is the number of Pareto optimal solutions. The smaller value of SP indicates that Pareto optimal solution distribution is more homogenized.

4.4. Result Analysis. In order to eliminate the contingency, each algorithm is run 30 times independently. The statistical results of the evaluation indexes are shown in Tables 2 and 3. In order to reflect the advantages and disadvantages of the optimization results more directly, the boxplots of GD value and SP value of each algorithm are given as in Figures 5 and 6.

The best optimal results of the algorithms in repeated experiments are shown in Figures 7, 8, and 9. The comparison is more intuitive.

For UF3 test problem, the sMOGWO, NSGA-III, and SPEA2 are the first class in GD value which means the solutions of these methods are closer to the real Pareto front. The GD values of MOPSO, MOGWO, and MOEA/D are high and fluctuating. The sMOGWO method has a better SP value which means the solutions are well distributed. Although the NSGA-III and SPEA2 are closer to the real Pareto front, the SP values are high, which means the solutions of these methods tend to fall into local optimum. We can discover that the NSGA-III and SPEA2 methods fall into local optimum on UF3 test problem intuitively according to Figure 7. The solutions of the sMOGWO method are the best.

For UF4 test problem, the sMOGWO has the best GD value. The MOPSO, MOGWO, and MOEA/D are in the second class in GD value. The sMOGWO, MOGWO, and MOPSO are in the first class in SP value. From Figure 8, the best optimal results of sMOGWO, MOPSO, MOGWO, and MOEA/D are all close to the real Pareto front and are well distributed.

For UF7 test problem, the GD values of sMOGWO, MOGWO, NSGA-III, and SPEA2 are in the first class, but the SP value of sMOGWO is better than those of other methods. From Figure 9, the best optimal result of all the

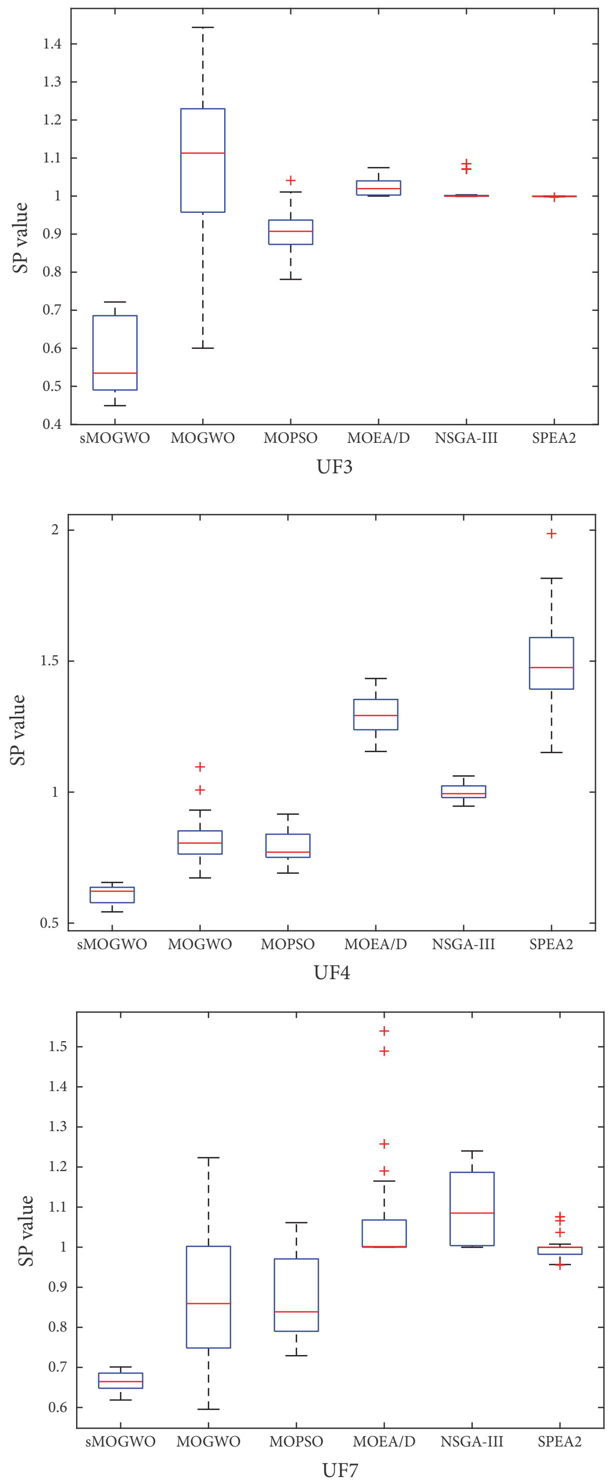

Figure 6: The boxplots of SP value of three algorithms.

methods is close to the real Pareto front, but the solutions of MOPSO, MOGWO, MOEA/D, NSGA-III, and SPEA2 are not well distributed. Some methods fall into local optimum. The solutions of the sMOGWO method are the best.

Accordingly, the proposed sMOGWO algorithm has good stability under all test functions, and the proposed algorithm performs well in repeated experiments with few poor results.

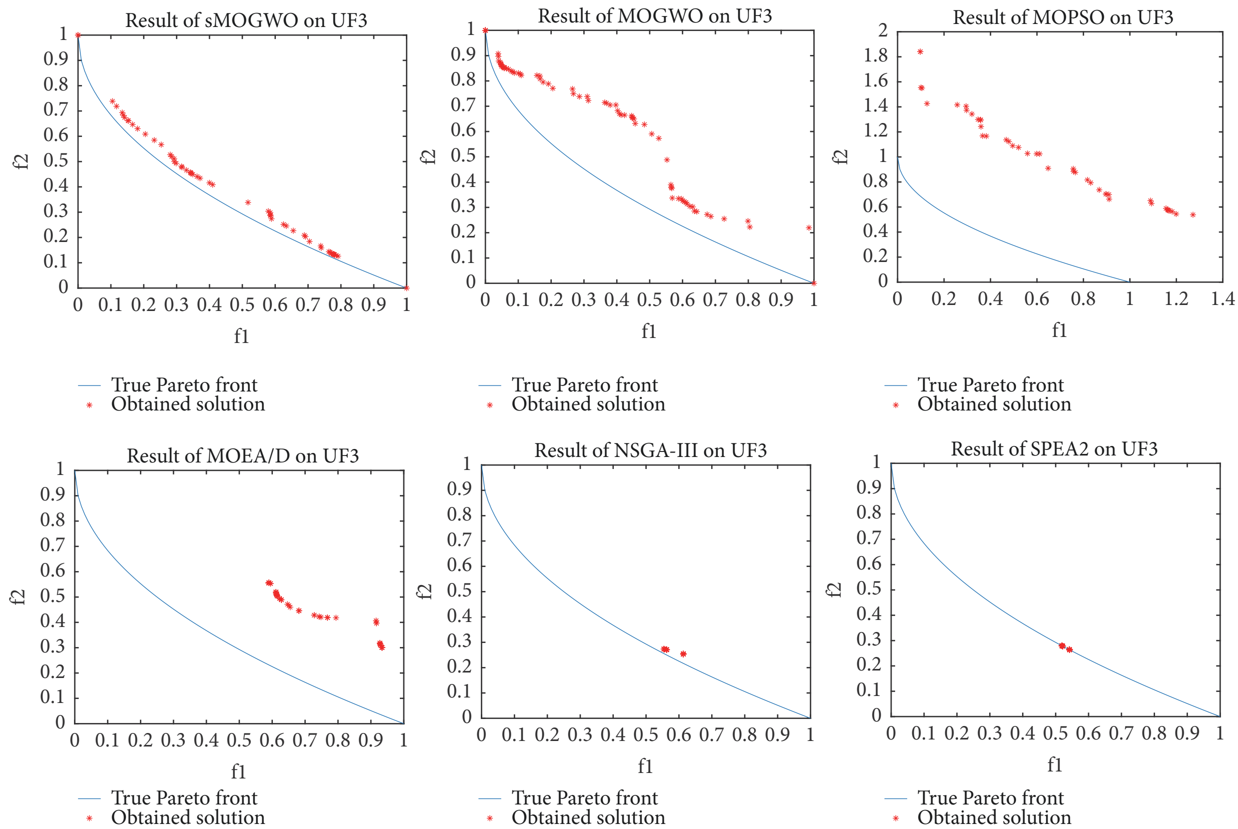

FIGURE 7: The best optimal results of the different algorithms in repeated experiments on UF3.

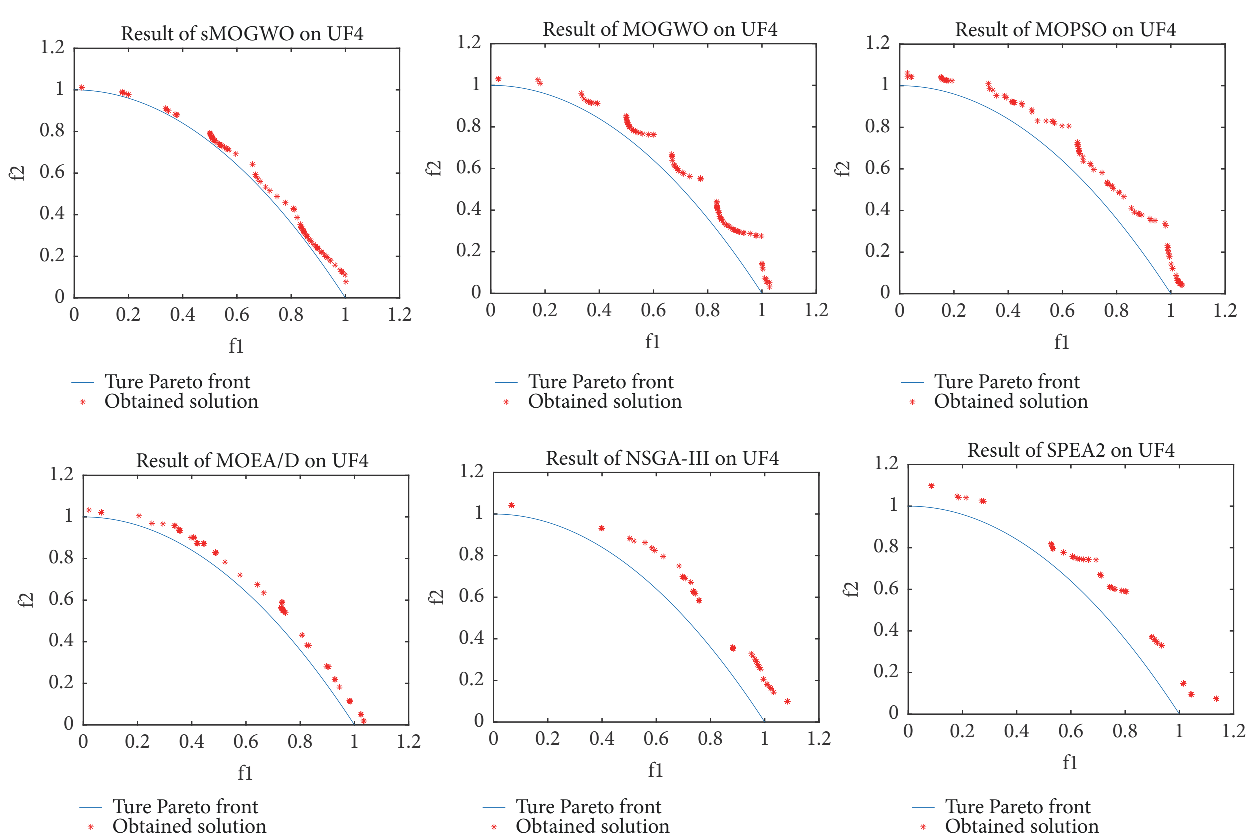

FIGURE 8: The best optimal results of the different algorithms in repeated experiments on UF4.

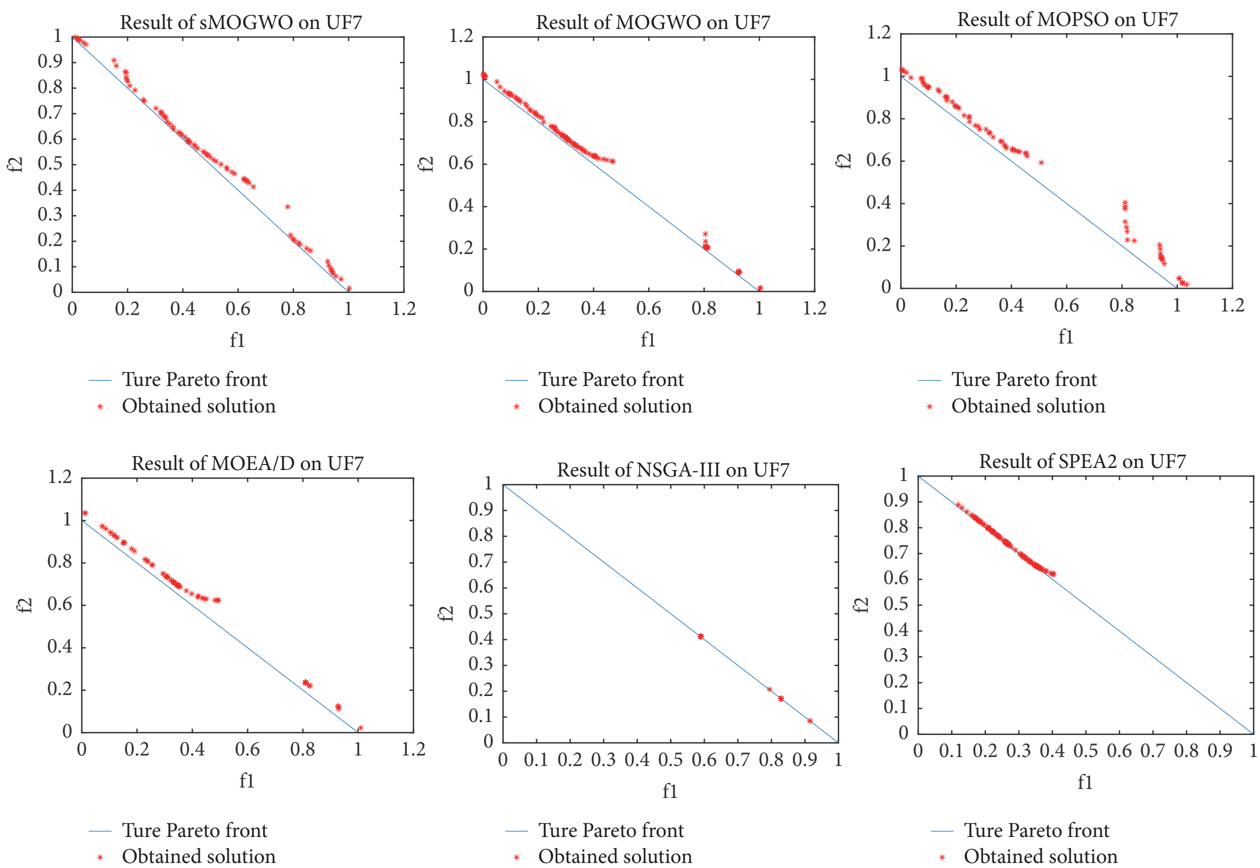

Figure 9: The best optimal results of the different algorithms in repeated experiments on UF7.

Table 4: Some representative control strategies are chosen from the Pareto optimal solution set.

Control strategy	Parameters of HGTS			Performance indexes	
	K_p	K_i	K_d	ITAE under no-load	ITAE under on-load
1	8.750	5.173	1.921	0.2352	0.0176
2	9.352	4.612	1.602	0.2156	0.0220
3	9.791	3.864	1.216	0.1925	0.0311
4	10.171	3.514	1.028	0.1752	0.0402
5	10.473	3.191	0.759	0.1585	0.0517
6	10.967	2.595	0.271	0.1284	0.0823

5. Case Study

In this section, a case study is presented to show the effect of the proposed algorithm on optimal control of HTGS under multiple operation conditions.

The no-load and on-load operation conditions are considered. The model of HTGS and its parameters are provided in Section 2. The multiobjective functions refer to (5) and (6). The simulation time is 20 seconds. The sMOGWO, MOGWO, MOPSO, MOEA/D, NSGA-III, and SPEA2 algorithms are utilized for optimal control. The maximum number of iterations is 100. The other parameters of the three algorithms are set as in Table 1. Each algorithm is run 30 times independently. The best optimal results of each algorithms in repeated experiments are shown in Figure 10.

The solutions of MOPSO method are far away from Pareto front. The solutions of sMOGWO, MOGWO, MOPSO, MOEA/D, NSGA-III, and SPEA2 are similar to the Pareto front, but the solutions of sMOGWO are more evenly distributed than those of other methods.

In order to analyze the detailed control transient process of the optimization results, some representative control strategies are chosen from the Pareto optimal solution set as shown in Table 4. It can be seen that the optimization of ITAE under no-load and ITAE under on-load are opposites. Transient process of some of the control strategies is shown in Figure 11 to exhibit control effects more intuitively.

All the three control strategies have good control stability under multiple operation conditions. Strategy 1 is most stable

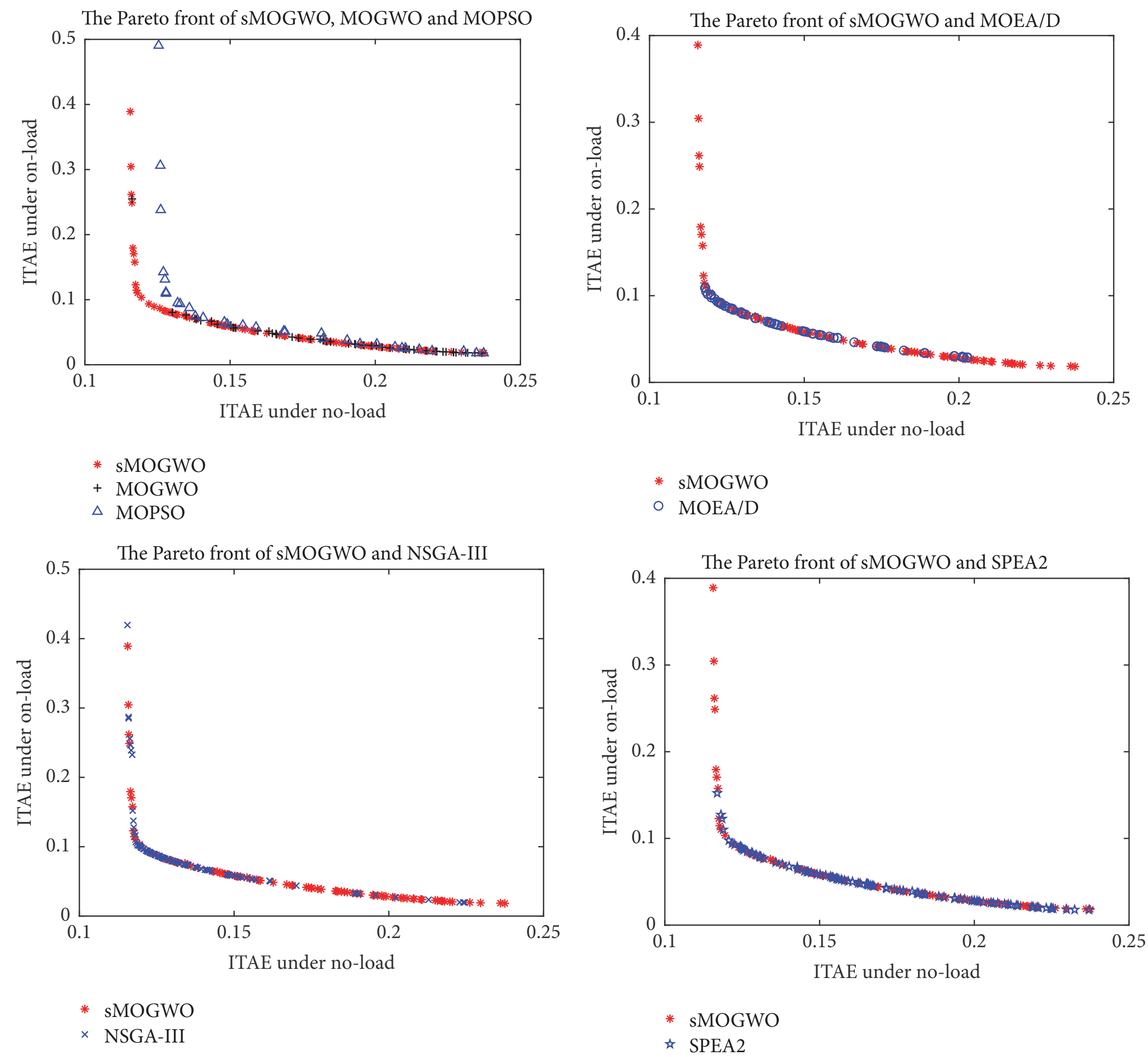

Figure 10: The Pareto front of different algorithms.

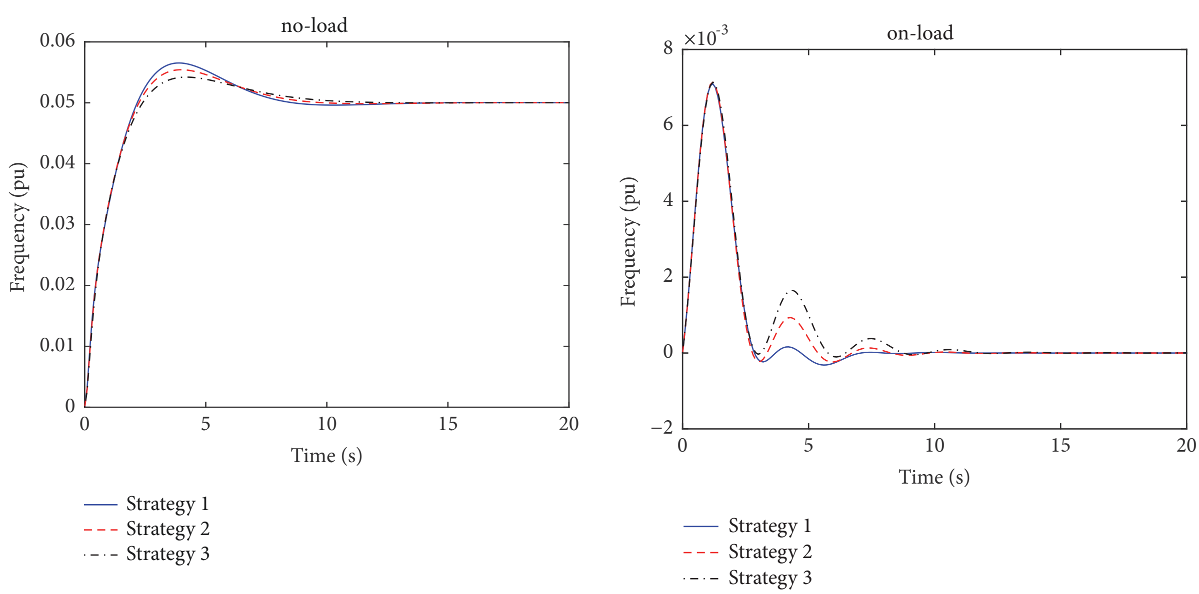

Figure 11: Transient process by different control strategies.

under on-load operation condition, but it has bigger overshoot than the other two strategies under no-load operation condition. Strategy 3 has the smallest overshoot among the three strategies under no-load operation condition, but its stability is the worst among the control strategies under on-load operation condition. Strategy 2 is a compromise control strategy.

Thus, a Pareto solution set can be got after one optimization which can be suitable for multiple operation conditions. And the solutions have different emphasis on objective functions. According to the specific requirements of the HTGS, the decision maker can select one or some satisfactory solutions from this solution set as the final solution, so that the HTGS can obtain better control quality.

6. Conclusion

The control strategies of hydraulic turbine governing system need to consider the multiple operation conditions. A multi-objective optimal function under different operation conditions is proposed in this paper to solve this control problems.

In order to optimize the multiobjective problems more effectively, a novel MOGWO algorithm based on searching factor (sMOGWO) is proposed. The sMOGWO method is verified with several UF test problems compared to MOGWO, MOPSO, MOEA/D, NSGA-III, and SPEA2. The sMOGWO provided better solution compared with its competitors. And the proposed algorithm has good stability under all test functions, and the proposed algorithm performs well in repeated experiments with few poor results.

A case study has been designed to test the control quality of the control strategies which are got by the proposed method. The experimental results have confirmed that the control strategies perform well under multiple operation conditions.

Data Availability

The simulation data used to support the findings of this study are available from the corresponding author upon request.

Conflicts of Interest

We declare that we have no conflicts of interest regarding the publication of this manuscript.

Acknowledgments

This paper is supported by the National Natural Science Foundation of China (no. 51709121, no. 51709122) and Six Talent Peaks Project of Jiangsu Province of China (no. RJFW-028).

References

[1] F. J. Tapiador, "Assessment of renewable energy potential through satellite data and numerical models," *Energy & Environmental Science*, vol. 2, no. 11, pp. 1142–1161, 2009.

[2] W. Fu, K. Wang, C. Li, and J. Tan, "Multi-step short-term wind speed forecasting approach based on multi-scale dominant ingredient chaotic analysis, improved hybrid GWO-SCA optimization and ELM," *Energy Conversion and Management*, vol. 187, pp. 356–377, 2019.

[3] H. Price, E. Lüpfert, D. Kearney et al., "Advances in parabolic trough solar power technology," *Journal of Solar Energy Engineering*, vol. 124, no. 2, pp. 109–125, 2002.

[4] H. Shaker, H. Zareipour, and D. Wood, "Impacts of large-scale wind and solar power integration on California's net electrical load," *Renewable & Sustainable Energy Reviews*, vol. 58, pp. 761–774, 2016.

[5] J. Widén, "Correlations between large-scale solar and wind power in a future scenario for Sweden," *IEEE Transactions on Sustainable Energy*, vol. 2, no. 2, pp. 177–184, 2011.

[6] R. Mukund Patel, "Impacts of large-scale solar and wind power production on the balance of the swedish power system," in *Proceedings of the World Renewable Energy Congress – Sweden*, pp. 851–858, 2011.

[7] X. Lai, C. Li, J. Zhou, and N. Zhang, "Multi-objective optimization of the closure law of guide vanes for pumped storage units," *Journal of Renewable Energy*, vol. 139, pp. 302–312, 2019.

[8] C. Li, W. Wang, and D. Chen, "Multi-objective complementary scheduling of hydro-thermal-RE power system via a multi-objective hybrid grey wolf optimizer," *Energy*, vol. 171, pp. 241–255, 2019.

[9] E. Ivanova, R. Malti, and X. Moreau, "Time-domain simulation of MIMO fractional systems," *Nonlinear Dynamics*, vol. 84, no. 4, pp. 2057–2068, 2016.

[10] C. Zhihuan, Y. Xiaohui, J. Bin, P. Wang, and T. Hao, "Design of a fractional order PID controller for hydraulic turbine regulating system using chaotic non-dominated sorting genetic algorithm II," *Energy Conversion & Management*, vol. 84, pp. 390–404, 2014.

[11] C. Li, J. Zhou, L. Chang, Z. Huang, and Y. Zhang, "T-S fuzzy model identification based on a novel hyperplane-shaped membership function," *IEEE Transactions on Fuzzy Systems*, vol. 25, no. 5, pp. 1364–1370, 2017.

[12] X. Yu, F. Yang, Y. Huang, and H. Nan, "Fuzzy immune sliding mode control based hydro turbine governor," in *Proceedings of the Third International Conference on Natural Computation (ICNC 2007)*, pp. 171–176, Haikou, China, August 2007.

[13] K. Ro and H.-H. Choi, "Application of neural network controller for maximum power extraction of a grid-connected wind turbine system," *Electrical Engineering*, vol. 88, no. 1, pp. 45–53, 2005.

[14] D. Qian, J. Yi, X. Liu, and X. Li, "GA-based fuzzy sliding mode governor for hydro-turbine," in *Proceedings of the International Conference on Intelligent Control and Information Processing (ICICIP '10)*, pp. 382–387, Dalian, China, August 2010.

[15] A. Panwar, G. Sharma, I. Nasiruddin, and R. C. Bansal, "Frequency stabilization of hydro power system using hybrid bacteria foraging PSO with UPFC and HAE," *Electric Power Systems Research*, vol. 161, pp. 74–85, 2018.

[16] Z. Chen, X. Yuan, H. Tian, and B. Ji, "Improved gravitational search algorithm for parameter identification of water turbine regulation system," *Energy Conversion & Management*, vol. 78, no. 30, pp. 306–315, 2014.

[17] C. Li, N. Zhang, X. Lai, J. Zhou, and Y. Xu, "Design of a fractional-order PID controller for a pumped storage unit using a gravitational search algorithm based on the Cauchy and

Gaussian mutation," *Information Sciences*, vol. 396, pp. 162–181, 2017.

[18] T. Tian, C. Liu, Q. Guo, Y. Yuan, W. Li, and Q. Yan, "An improved ant lion optimization algorithm and its application in hydraulic turbine governing system parameter identification," *Energies*, vol. 11, no. 1, article no 95, 2018.

[19] K. Deb, A. Pratap, S. Agarwal, and T. Meyarivan, "A fast and elitist multiobjective genetic algorithm: NSGA-II," *IEEE Transactions on Evolutionary Computation*, vol. 6, no. 2, pp. 182–197, 2002.

[20] X. Bi and C. Wang, "An improved NSGA-III algorithm based on objective space decomposition for many-objective optimization," *Soft Computing*, vol. 21, no. 15, pp. 4269–4296, 2017.

[21] Q. Zhang and H. Li, "MOEA/D: a multiobjective evolutionary algorithm based on decomposition," *IEEE Transactions on Evolutionary Computation*, vol. 11, no. 6, pp. 712–731, 2007.

[22] A. Wahid, X. Gao, and P. Andreae, "Multi-objective clustering ensemble for high-dimensional data based on Strength Pareto Evolutionary Algorithm (SPEA-II)," in *Proceedings of the IEEE International Conference on Data Science and Advanced Analytics, (DSAA '15)*, France, October 2015.

[23] C. A. Coello Coello and M. S. Lechuga, "MOPSO: a proposal for multiple objective particle swarm optimization," in *Proceedings of the Congress on Evolutionary Computation (CEC '02)*, pp. 1051–1056, May 2002.

[24] H. Borhanazad, S. Mekhilef, V. Gounder Ganapathy, M. Modiri-Delshad, and A. Mirtaheri, "Optimization of micro-grid system using MOPSO," *Journal of Renewable Energy*, vol. 71, pp. 295–306, 2014.

[25] S. Mirjalili, S. Saremi, S. M. Mirjalili, and L. D. S. Coelho, "Multi-objective grey wolf optimizer: A novel algorithm for multi-criterion optimization," *Expert Systems with Applications*, vol. 47, pp. 106–119, 2016.

[26] G. Karer and S. Igor, "Interval-model-based global optimization framework for robust stability and performance of PID controllers," *Applied Soft Computing*, vol. 40, pp. 526–543, 2016.

[27] S. Mirjalili, S. M. Mirjalili, and A. Lewis, "Grey wolf optimizer," *Advances in Engineering Software*, vol. 69, no. 3, pp. 46–61, 2014.

[28] K. Li, R. Wang, T. Zhang, and H. Ishibuchi, "Evolutionary many-objective optimization: a comparative study of the state-of-the-art," *IEEE Access*, vol. 6, pp. 26194–26214, 2018.

[29] P. A. Grudniewski and A. J. Sobey, "Multi-Level Selection Genetic Algorithm applied to CEC 09 test instances," in *Proceedings of the IEEE Congress on Evolutionary Computation, (CEC '17)*, pp. 1613–1620, Spain, June 2017.

[30] Y. Chen, C. Cheng, S. Li, and C. Yu, "Location optimization for multiple types of charging stations for electric scooters," *Applied Soft Computing*, vol. 67, pp. 519–528, 2018.